Electronic Supplementary Information

Direct electrochemistry and electrocatalysis of glucose oxidase-functionalized bioconjugate as a trace label for ultrasensitive detection of thrombin

Lijuan Bai, Ruo Yuan*, Yaqin Chai, Yali Yuan, Yan Wang, Shunbi Xie

Education Ministry Key Laboratory on Luminescence and Real-Time Analysis, College of Chemistry and Chemical Engineering, Southwest University, Chongqing 400715, People's Republic of China

EXPERIMENTAL SECTION

Reagents and Materials

Graphene oxide (GO) was obtained from Nanjing xianfeng nano Co. (China). N-hydroxy succinimide (NHS) and 1-ethyl-3-(3-dimethylaminopropyl) carbodiimide hydrochloride (EDC) were acquired from Shanghai Medpep Co. (China). Shortened carboxylate carbon nanotubes (CNTs), poly(amino-amine) dendrimers (PAMAM), thrombin, glucose oxidase (GOD), dimethyl formamide (DMF) and chloroplatinic acid (H_2PtCl_6) were purchased from Sigma-Aldrich Chemical Co. (USA). Poly(diallyldimethylammonium chloride) (PDDA) were obtained from Beijing Chemical Reagent Co. (China). Thrombin binding aptamer (TBA): 5'-NH_2-$(CH_2)_6$-GGTTGGTGTGGTTGG-3' was purchased from TaKaRa (China). Trishydroxymethylaminomethane hydrochloride (Tris-HCl) was supplied by Roche (Switzerland). 0.1 M phosphate buffered solutions (PBS, pH 7.0) containing 10 mM Na_2HPO_4, 10 mM KH_2PO_4 and 2 mM $MgCl_2$ was used as working buffer. 20 mM Tris-HCl buffer (pH 7.4) containing 140 mM NaCl, 5 mM KCl, 1 mM $CaCl_2$ and 1 mM $MgCl_2$ was used as binding buffer. All other chemicals were of reagent grade and used as received.

Apparatus and characterization

Cyclic voltammetry (CV) and differential pulse voltammetry (DPV) measurements were carried out with a CHI 610A electrochemical workstation (Shanghai Chenhua Instrument, China). All experiments were performed in a conventional three-electrode system: a platinum wire auxiliary electrode, a saturated calomel reference electrode (SCE) and the modified glassy carbon electrode (GCE, Φ = 4mm) as working electrode. The scanning electron micrographs were taken with scanning electron microscope (SEM, S-4800, Hitachi, Japan). X-ray photoelectron spectroscopy (XPS) analysis was carried out using a VG Scientific ESCALAB 250 spectrometer, using Al Kα X-ray (1486.6 eV) as the light source. The pH measurements were made with a pH meter (MP 230, Mettler-Toledo, Switzerland).

Preparation of PtNPs decorated rGO nanocomposite (PtNPs@rGO)

Initially, reduced graphene oxide (rGO) was prepared according to reference[1] with a slight modification. 0.2 mL PDDA (30%) was added to 50 mL stable dispersion of exfoliated graphene oxide (GO) sheets (1 mg mL^{-1}) and stirred for 30 min. Then 0.5 mL hydrazine hydrate (80%) was added and heated under stirring at 90 °C for about 12 h. The obtained black rGO was washed several times by double distilled water and collected by centrifugation. Platinum nanoparticles (PtNPs) were attached to rGO by electrostatic adsorption between the positively charged rGO and the negatively charged PtNPs, using $NaBH_4$ reduction method. Briefly, 1 mL H_2PtCl_6 (1%) was added dropwise into 5 mL rGO suspension and vigorously stirred for 5 min to make the negatively charged $PtCl_6^{2-}$ ions adsorbed on the rGO surface. Then, 2.5 mL $NaBH_4$ (0.1 M) solution was dropped into the mixture with stirring for 30 min, followed by centrifugation and washing with double distilled water.

Preparation of GOD and TBA labeled PtNPs@rGO (TBA-GOD-PtNPs@rGO) bioconjugate

It is reported that PtNPs have strong adsorption ability of thiol and amino groups.[2] Thus, the

TBA-GOD-PtNPs@rGO bioconjugate was synthesized according to the following steps. Firstly, 5 mL of the above PtNPs@rGO suspension was mixed with 0.1 mL amino TBA (2 μM) and incubated at 4 °C for 12 h under softly stirring. Subsequently, 1 mL GOD (10 mg mL^{-1}) with abundant thiol and amino groups was added into the PtNPs@rGO labeled TBA solution and incubated for 24 h at 4 °C. After centrifugation and washing, the TBA-GOD-PtNPs@rGO bioconjugate was resuspened in Tris-HCl buffer and stored at 4 °C for further use.

Experimental measurements

Electrochemical experiments were carried out in a conventional electrochemical cell, in which a modified working electrode, a SCE reference electrode and a Pt counter electrode were used. CV measurements were taken from -0.7 to -0.15 V (vs. SCE) at a scan rate of 100 mV s^{-1} in 0.1 M PBS (pH 7.0). DPV measurements were performed in 0.1 M PBS (pH 7.0) containing appropriate amount of glucose to measure the amperometric responses of the aptasensor. The parameters applied were: 50 mV pulse amplitude, 50 ms pulse width, 0.2 s pulse period and voltage range from -0.1 to -0.7 V (vs. SCE).

RESULTS AND DISCUSSION

Characteristics of the different nanomaterials

Scanning electron microscopy (SEM) images were taken to observe the morphological features of the as synthesized samples. As shown in Fig. S1a, CNTs and PAMAM dispersed in DMF showed a homogeneous configuration and good dispersion, which presented a large specific surface area and good biocompatibility for the immobilization of aptamers. The large lamellate and scrolled sheets suggested the successful preparation of rGO (Fig. S1b). The homogeneous and dense coverage of PtNPs on the rGO could be observed in Fig. S1c, implying the successful synthesis of PtNPs@rGO. The sheets and nanoparticles remained separated with each other without any aggregation, implying the well dispersibility of the nanocomposite in solution.

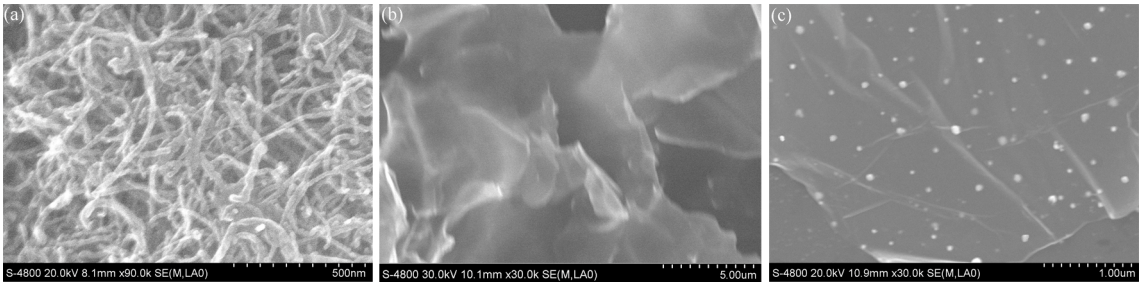

Fig. S1 SEM images of PAMAM-CNTs (a), rGO (b) and PtNPs@rGO (c).

To further analyze the chemical composition of different nanomaterials, XPS characterization was employed. Fig. S2a and Fig. S2b showed the C1s and O1s core level spectrum of GO. Fig. S2c represented the XPS signature of the Pt4f doublet (71.1eV and 74.4eV) for the resulting metallic Pt^0, which suggesting the form of PtNPs on rGO. The N1S core level spectrum in Fig. S2d mainly originated from GOD. In addition, the fully scanned spectra in Fig. S2e also confirmed that the GOD-PtNPs@rGO bioconjugate have been successfully prepared.

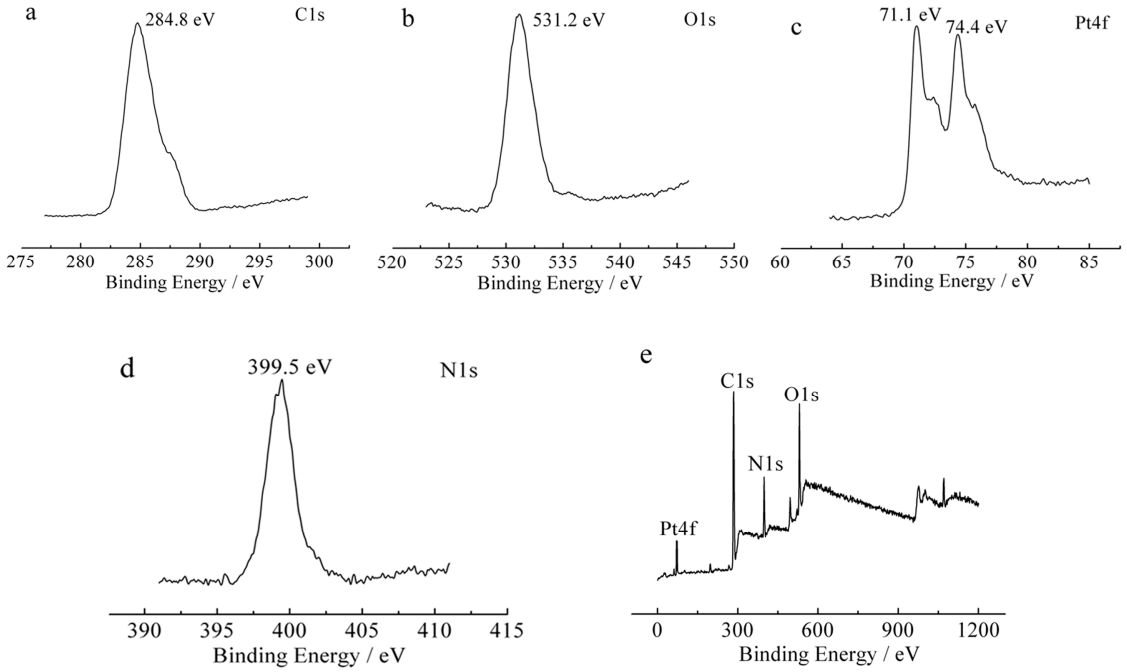

Fig. S2 XPS analysis of different nanomaterials. (a) and (b) were the C1s and O1s core level spectrum of GO; (c) was the Pt4f core level spectrum of PtNPs on rGO; (d) and (e) were the N1s core level spectrum in GOD and coverage of GOD-PtNPs@rGO nanocomposite.

The electroactive surface area of PAMAM-CNTs modified electrode

In order to illustrate that the prepared PAMAM-CNTs nanohybrid film could improve the surface area and conductivity of the aptasensor, electroactive surface area (A) of ordinary gold nanoparticles (AuNPs) modified electrode and PAMAM-CNTs modified electrode was determined by CV in 5.0 mM $Fe(CN)_6^{4-/3-}$ solution containing 0.1 M KCl at different sweep rates (v) according to the Randles-Sevcik equation:[3] $Ip = 2.69 \times 10^5 A \times D^{1/2} n^{3/2} v^{1/2} C$. As shown in Fig. S3a and Fig. S3b, both the peak currents (Ip) of AuNPs modified electrode and PAMAM-CNTs modified electrode were proportional to the square root of scan rate. Therefore, with the constant parameters of D, C and n, we could successfully obtain an approximate value of A according to the Randles-Sevcik equation. The electroactive surface area of 16.98 mm^2 and 24.25 mm^2 for AuNPs modified electrode and PAMAM-CNTs modified electrode were acquired, respectively. The electroactive surface area of PAMAM-CNTs modified electrode increased about 42.8% compared with AuNPs modified electrode, which provided an effective evidence for the superior conductivity of PAMAM-CNTs film as expected.

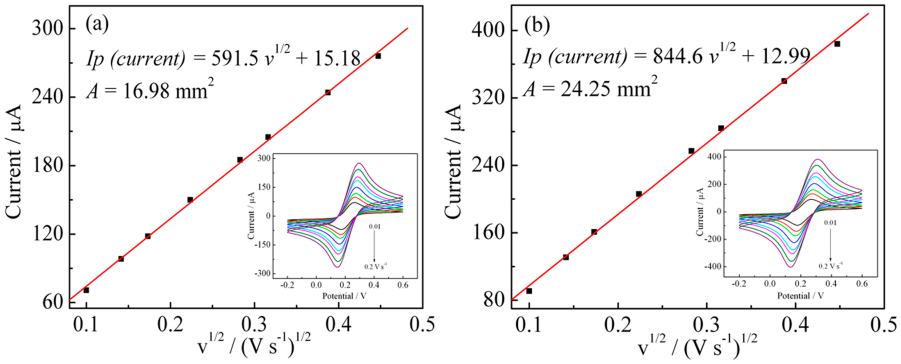

Fig. S3 CVs of bare GCE (a) and PAMAM-CNTs modified GCE (b) in 5.0 mM $Fe(CN)_6^{4-/3-}$ at different scan rates from 10 to 200 mV s^{-1}. Insets were the linear relations of bare and PAMAM-CNTs modified GCE with the anodic peak current against the square root of scan rate.

DET of GOD and the comparison of different signal amplification strategies

In order to prove that the direct electron transfer originated from GOD, two kinds of TBA functionalized label were prepared and the results are shown in Fig. S4(A). No redox peak was

observed (curve a) because of the lack of GOD. The well-defined redox peak (curve b) originated from the reversible redox reaction of GOD: GOD(FAD) + $2e^-$ +$2H^+$ ↔ GOD($FADH_2$), where FAD and $FADH_2$ are the oxidized and reduced forms of the GOD redox center, respectively.[4] The separation of peak potentials (ΔEp) is 40 mV, indicating that the redox center (FAD/$FADH_2$) of GOD immobilized on PtNPs@rGO could display a quasi-reversible electrochemical reaction despite its large molecular structure. The apparent heterogeneous electron transfer rate constant (k_s) was estimated to be 2.6 s^{-1} from the dependence of ΔEp on the scan rates.[5] The value was higher than that (1.53 s^{-1}) reported previously at PPMH modified electrode,[6] suggesting that direct electron transfer of GOD on PtNPs@rGO had good reversibility.

As shown in Fig. S4(B), the proposed aptasensor (curve c) had a much higher current response than that without CNTs as sensor platform (curve a), indicating CNTs with hollow and tubal structure provided electron transfer tunnels and could facilitate the electron transfer between GOD and electrode. The aptasensor using the trace label without rGO (curve b) also showed a smaller current response than the proposed aptasensor, implying rGO with large accessible surface area could enhance the immobilization of GOD, thus amplifying the electrochemical signal.

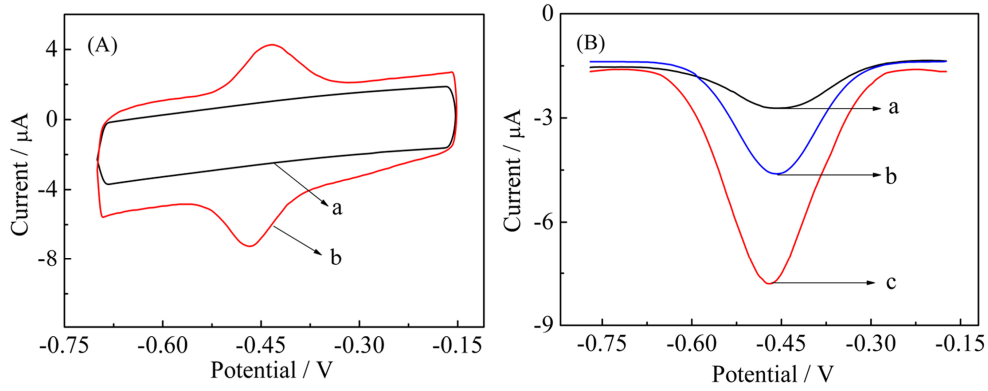

Fig. S4 (A) CVs of the resulted aptasensor after the sandwich reaction with (a) TBA-PtNPs@rGO label and (b) TBA-GOD-PtNPs@rGO label. (B) DPVs of (a) TBA-GOD-PtNPs@rGO/TB/TBA/PAMAM/GCE, (b) TBA-GOD-PtNPs/TB/TBA/PAMAM-CNTs/GCE and (c) TBA-GOD-PtNPs@rGO/TB/TBA/PAMAM-CNTs/GCE in

0.1 M PBS (pH 7.0) containing 4.2 mM glucose.

Optimization of the modified TBA concentration

In order to obtain a higher sensitivity of the electrochemical aptasensor, the modified TBA concentration was optimized. 20 μL of TBA with different concentrations was attached onto the PAMAM-CNTs modified electrode and measured in 5.0 mM $Fe(CN)_6^{4-/3-}$. As shown in Fig. S4, the peak current decreased with the increasing of the modified TBA concentration, and reached plateau regions at the concentration of 2 μM. Thus, the optimal TBA concentration was chosen at 2 μM.

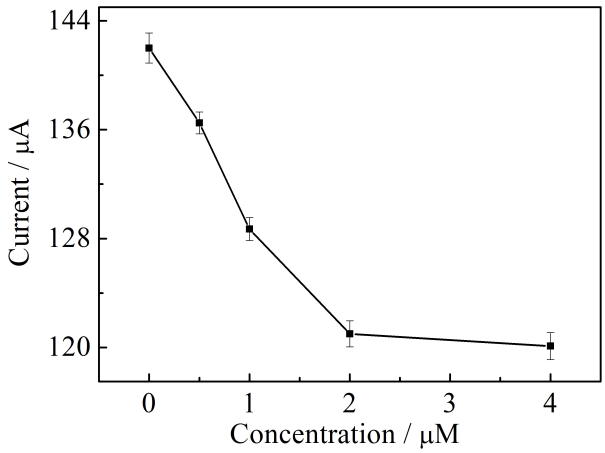

Fig. S5 Optimization of the modified TBA concentration.

Comparisons of proposed aptasensor with other detection methodologies for thrombin detection

Table S1 Performance compared with other detection methodologies for thrombin detection.

Analytical method	Linear range (M)	Detection limit (M)	Ref.
Differential pulse voltammetry	5.0×10^{-12} – 7.0×10^{-9}	3.0×10^{-12}	7
Quartz crystal microbalance	5.0×10^{-10} – 1.3×10^{-8}	1.0×10^{-10}	8
Electrochemical impedance spectroscopy	5.0×10^{-11} – 1.8×10^{-8}	2.0×10^{-11}	9
Electrochemiluminescent	3.3×10^{-13} – 3.3×10^{-11}	2.0×10^{-13}	10
Differential pulse voltammetry	1.0×10^{-12} – 3.0×10^{-8}	3.9×10^{-13}	11
Fluorescence	5.0×10^{-10} – 2.0×10^{-8}	1.8×10^{-10}	12
Differential pulse voltammetry	3.0×10^{-13} – 3.5×10^{-8}	2.1×10^{-13}	Present work

Analytical application of the aptasensor

To further investigated the analytical reliability and possible application of the proposed aptasensor, recovery experiments were performed by standard addition methods in human serum. A series of samples were prepared by adding thrombin of different concentrations into healthy human serum samples. As shown in Table S2, the recovery was between 94.6% and 108.1%. These results indicated that the proposed electrochemical aptasensor provided a potential application in real biological samples.

Table S2. Determination of thrombin added in human serum with the proposed aptasensor

Serum samples	Added thrombin (M)	Found thrombin (M)[a]	Relative standard deviation (%)	Recovery (%)
1	10^{-12}	1.01×10^{-12}	4.2	105.3
2	10^{-11}	9.46×10^{-10}	5.9	94.6
3	10^{-10}	9.97×10^{-9}	7.1	99.7
4	10^{-9}	1.08×10^{-9}	6.4	108.1
5	10^{-8}	1.04×10^{-8}	5.3	103.8

[a] Calculated as a mean of three measurements.

Performance of the aptasensor for PDGF detection

The performance of the present aptasensor was evaluated by detecting PDGF standard solutions with the DPV technique under the optimization conditions according to the typical procedure for sandwich-type reaction. As expected for a sandwich mechanism, the catalytic cathodal peak current density of the aptasensor increased with the increasing PDGF concentrations (Fig. S6a). The linear range spaned the concentration of PDGF from 2.0×10^{-13} to 3.0×10^{-8} M with a detection limit of 1.5×10^{-13} M (Fig. S6b), which proved the proposed aptasensor could be successfully used for the detection of other proteins.

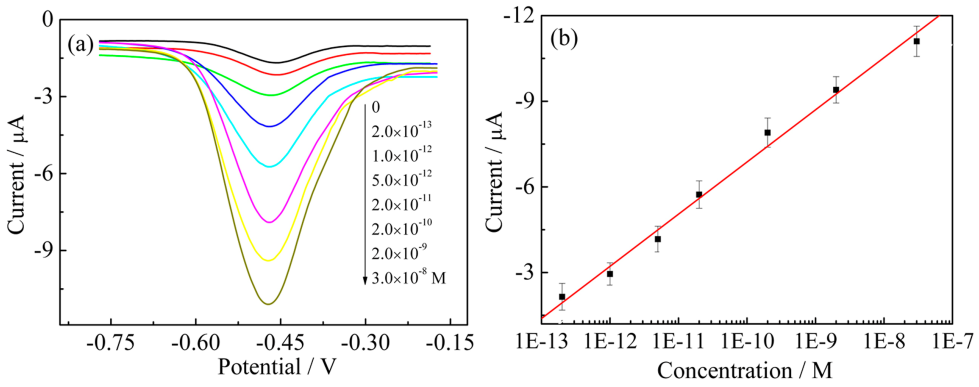

Fig. S6 (a) DPV responses of the proposed aptasensor for PDGF detection at different concentrations in 0.1 M PBS (pH 7.0) containing 4.2 mM glucose. (b) The calibration curve of electrocatalytic current response versus PDGF with various concentrations.

References

1 L. L. Li, K. P. Liu, G. H. Yang, C. M. Wang, J. R. Zhang, J. J. Zhu. *Adv. Funct. Mater.*, 2011, **21**, 869.

2 T. Y. You, O. Niwa, M. Tomita, S. Hirono. *Anal. Chem.*, 2003, **75**, 2080; R. Polsky, R. Gill, L. Kaganovsky, I. Willner. *Anal. Chem.*, 2006, **78**, 2268.

3 A. J. Bard, L. R. Faulkner. Electrochemical methods: fundamentals and applications, 2nd ed., Wiley, New York, 1980.

4 Y. Wang, Y. Y. Shao, D. W. Matson, J. H. Li, Y. H. Lin. *ACS Nano*, 2010, **4**, 1790; P. Si, S. J. Ding, J. Yuan, X. W. Lou, D. H. Kim. *ACS Nano*, 2011, **5**, 7617.

5 E. Laviron. *J. Electroanal. Chem.*, 1979, **101**, 19.

6 Y. Oztekin, A. Ramanaviciene, Z. Yazicigil, A. O. Solak, A. Ramanavicius. *Biosens. Bioelectron.*, 2011, **26**, 2541.

7 Y. C. Fu, T. Wang, L. J. Bu, Q. J. Xie, P. H. Li, J. H. Chen, S. Z. Yao. *Chem. Commun.*, 2011, **47**, 2637.

8 Q. Chen, W. Tang, D. Z. Wang, X. J. Wu, N. Li, F. Liu. *Biosens. Bioelectron.*, 2010, **26**, 575.

9 B. L. Li, Y. L. Wang, H. Wei, S. J. Dong. *Biosens. Bioelectron.*, 2008, **23**, 965.

10 Z. Y. Lin, L. F. Chen, X. Zhu, B. Qiu, G. N. Chen. *Chem. Commun.*, 2010, **46**, 5563.

11 L. J. Bai, R. Yuan, Y. Q. Chai, Y. L. Yuan, Y. Zhuo, L. Mao. *Biosens. Bioelectron.*, 2011, **26**, 4331.

12 Y.H. Wang, L. Bao, Z.H. Liu, D.W. Pang. *Anal. Chem.*, 2011, **83**, 8130.